PCCP

Accepted Manuscript

ROYAL SOCIETY OF CHEMISTRY

www.rsc.org/pccp

Physical Chemistry Chemical Physics
CREATED USING THE RSC LaTeX PCCP ARTICLE TEMPLATE – SEE www.rsc.org/electronicfiles FOR DETAILS
ARTICLE TYPE www. rsc.org/xxxxxx | XXXXXXXX

Towards optimal seeding for the synthesis of ordered nanoparticle arrays on alumina/$Ni_3Al(111)$

Jimena A. Olmos-Asar,[a,b] Erik Vesselli,[c,d] Alfonso Baldereschi[a] and Maria Peressi*[,a,e]

Received Xth XXXXXXXXXX 20XX, Accepted Xth XXXXXXXXX 20XX
First published on the web Xth XXXXXXXXXX 20XX
DOI: 10.1039/b000000x

The adsorption and the nucleation of different transition metals (Fe, Co, Ni, Cu, Pd, Ag, Au) on alumina/$Ni_3Al(111)$ have been studied to shed light on the first stages of the synthesis of supported nanoparticles, focusing in particular on the possibility of producing ordered arrays. Affinity towards oxygen, atomic radii, electronic properties and kinetics have been taken into account to rationalize the different behavior. In agreement with empirical findings, Pd is confirmed to be the best choice for a highly ordered nucleation following the *"dot"* superstructure of the alumina, due to a remarkable preference for the corresponding adsorption sites (holes) with respect to others, and for a rather strong binding. Atom by atom nucleation of this material has been studied, for seeds up to 6 atoms that offer a stiff anchoring of nanoparticles to the support.

1 Introduction

Metal nanoparticles (NPs), as an intermediate state of matter between atoms in the gas phase and bulk materials, often exhibit exceptional physical and chemical properties, which appear as soon as surface, interface, and finite-size effects start to play a role. In the search for good catalysts, nanoparticles are usually interesting systems due to their high surface-to-volume ratio, and also to the high concentration of special sites as edges and kinks [1] where reactions tend to have lower activation energies.

For many applications clusters must be supported and in that case, the presence of the substrate can also determine and modify the particle behavior. Recent studies of oxide-supported metal nanoparticles show an enhanced catalytic activity of nanoclusters in the presence of oxide phases. [2–6]

The shape and size of a metallic NP define its properties. It is because of this reason that the synthesis of ordered arrays of well-defined equally sized nanoclusters is the goal of many efforts in view of the development of new electronic and optoelectronic devices. Such clusters arrays would also be helpful for the study of the basic mechanisms that determine the activity of heterogeneous catalysts.

Several methods have been successfully applied to nanofabrication, like electron beam lithography, deposition of colloidal particles, atomic manipulation with the scanning tunnelling microscope (STM) and laser-beam assisted deposition, among others. [7–9] All these techniques involve direct instrumental manipulations of the systems and are almost independent on the physical properties of the substrate.

In recent years, there has been increased interest in surface structures with a strong modulation of the potential energy surface that can serve as templates for growing regular arrays of NPs through self-assembly upon chemical vapour deposition (CVD), exploiting the intrinsic properties of the substrate, as strain-relief patterns or misfit dislocations. [10,11] This approach has the potential to achieve well-ordered nanoscale arrays in a single run, and the method is more efficient and reproducible. Nevertheless, it is limited to a certain choice of materials.

Among other substrates with intrinsic structural properties, ultrathin oxide films are interesting candidates. In particular, oxidation of the clean $Ni_3Al(111)$ surface under ultra high vacuum (UHV) conditions gives rise to a highly ordered, extremely homogeneous and almost defect-free ultrathin non-stoichiometric alumina film. [12–17] Its unit cell orientation and size is $(\sqrt{67} \times \sqrt{67})R12^\circ$ with respect to the supporting alloy with a sixfold rotational symmetry, and in STM two superstructures can be observed: a so-called "*dot*" structure with a lattice parameter of 4.1 nm and one bright spot per unit cell (sample voltage bias around +2.3 V) and a hexagonal "*network*" structure with a lattice parameter of 2.6 nm and three depressions per unit cell, two darker than the other (voltage bias around +3.2 V). There exists a $(\sqrt{3} \times \sqrt{3})R30^\circ$ relation between the two structures, [17–20] and both can act as nucleation patterns for the growth of metallic nanoclusters [21–25] by

[a] *Department of Physics, University of Trieste, Strada Costiera 11, 34151 Trieste, Italy*
[b] *Departamento de Matemática y Física, Facultad de Ciencias Químicas, Universidad de Córdoba, XUA5000 Córdoba, Argentina*
[c] *Department of Physics and CENMAT, University of Trieste, via Valerio 2, 34127 Trieste, Italy*
[d] *IOM-CNR Laboratory TASC, AREA Science Park, 34149 Basovizza (Trieste), Italy*
[e] *IOM-CNR National Simulation Center DEMOCRITOS, 34136 Trieste, Italy. E-mail: peressi@ts.infn.it*

self-assembly of the metal deposited through CVD. The "*dot*" structure is delimited by holes, big enough (diameter of about 6.4 Å) to trap, in principle, any kind of metallic atom, that can then act as a seed for further growth of NPs. This template is especially useful because it combines the possibility to grow three-dimensional clusters with large distances between the nucleation sites (4.1 nm or 2.6 nm), allowing for tuning the cluster size in an extended range.

The intrinsic properties of the well-ordered hexagonal superstructure of the alumina film grown on $Ni_3Al(111)$ appear to lead under defined experimental conditions to the sought system yielding ordered nucleation of metal clusters and the formation of monodisperse nanoparticles.

Experimentally, it has been reported that selected metallic species (like Pd, Cu) nucleate exclusively in the holes, generating a well-ordered array of clusters.[21,22,26,27] On the other hand, other species (like V) nucleate preferentially in the "*network*" structure sites.[22] Finally, many other species (like Fe, Co, Ag, Au, Mn) tend to nucleate at both, the "*dot*" and the "*network*" structures, giving rise to less ordered arrays.[21–23,25] Pd is the atom usually chosen to create the initial seeds, due to the fact that it attaches inside the defects, and after that the metal of interest is grown on top of these self-assembled seeds.[19,25]

Becker et al.[22] studied the nucleation of many metals in the low and high coverage regime. They reported that most metals show strong preference for initial nucleation at the "*dot*" structure, but in the high-coverage regime they behave differently: for instance, Ag and Au form large aggregates, while Cu forms small clusters with short range order corresponding to the "*dot*" superstructure. They suggest that cohesive energies, adhesion energies, and metal-oxide interactions may play an important role.

In this work we focus our attention to the very low coverage regime, and in particular to the seeding mechanism and the first stages of nucleation of different selected transition metal clusters on $Al_2O_3/Ni_3Al(111)$, giving a rationale for the different behavior of the metallic species when deposited through CVD and in particular for the peculiarity of Pd.

2 Computational details

Calculations were performed within the Density Functional Theory approach implemented in the Quantum-Espresso package[28] with available ultrasoft pseudopotentials.[29] For the exchange and correlation the spin unrestricted Generalized Gradient Approximation in the Perdew-Burke-Ernzerhof[30] implementation was used. For the selection of the plain waves, energy cutoffs of 30 and 240 Ry were chosen to describe the wave function and the electronic density, respectively, and the sampling of the first Brillouin zone was performed at the Γ point.

The alumina grown onto $Ni_3Al(111)$ at UHV conditions is a highly ordered non stoichiometric thin film. The repetition unit consists on a hexagonal cell limited in the corners by holes that reach the supporting metallic alloy. The oxide grows onto the Ni_3Al as four alternated ion layers: Al-O-Al-O (oxygen-terminated). The full structure of the system was determined using a combination of *ab initio* simulations and STM experiments.[19]

Considering in the unit cell two layers of the metallic alloy under the oxide, the full simulation system is composed by 1257 atoms (268 atoms in each layer of the alloy, and four oxide layers consisting of: 132 Al, 188 O, 188 Al and 213 O respectively). Due to the big size of the repetition cell for the calculations we have used the same model systems around the zones of interest as in Ref.[31]. Independently on the metal coverage for the nucleation of NPs, the size of the reduced models has been chosen large enough in order to describe correctly the environment around the adsorption sites of interest, minimizing the effects of the borders.

In all calculations, the metallic seeds and the borders of the hole in the oxide are relaxed, while the underlying alloy and the rest of the alumina were kept fixed. The complete periodic cell is shown in Figure 1; the reduced models are marked on it. Enough vacuum has been added in all cartesian coordinates to assure no interaction among the repeated images.

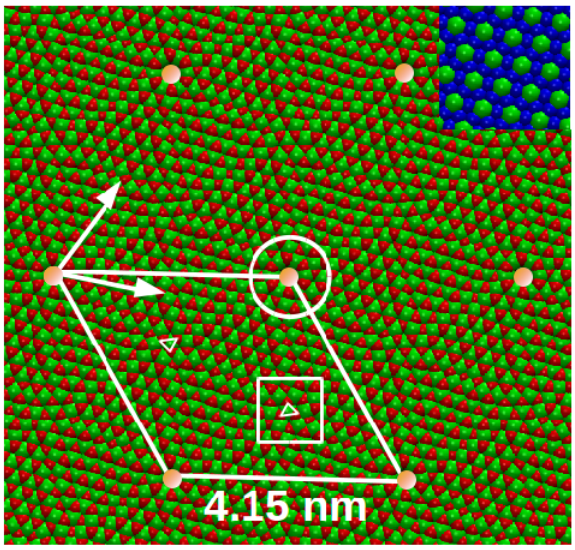

Fig. 1 Top view of the structural model of the $Al_2O_3/Ni_3Al(111)$, with the sketch of the periodically repeated unit cell. Directions of the primitive vectors of the underlying alloy are also indicated (a 2 nm × 2 nm portion is shown in inset). Orange spots highlight the *"dot"* structure and small triangles mark the *"network"*. The white circle and square identify the reduced models considered for calculations. Atomic coordinates are those obtained by Schmidt et al.[19] Red: O, green: Al, blue: Ni.

3 Results

3.1 Adsorption of metal atoms in the "*dot*" site

Motivated by the preferential adsorption of many metallic species in the "*dot*" and, to a less extent, in the "*network*" superstructure of the oxide, we have investigated the adsorption of seven transition metals (Me) in these two sites, starting from a single atom in the "*dot*". We have considered Fe, Co, Ni and Cu from the fourth period of the Periodic Table, Pd and Ag from the fifth, and Au from the sixth.

After optimization of the structure, the metal atom is in the bottom of the hole, as expected, interacting directly with the underlying Ni_3Al alloy, and in some cases slightly moves towards the borders of the hole, interacting also with the oxide. In Figure 2 the configurations and the adsorption energies, calculated as:

$$E^{Ads\ hole} = E_{Subs+Me} - E_{Subs} - E_{Me} \quad (1)$$

are shown. In this equation, $E_{Subs+Me}$ is the energy of the complete system, E_{Subs} is the energy of the supported alumina, and E_{Me} is the energy of an individual metal atom in vacuum. With this definition, negative values mean stabilization.

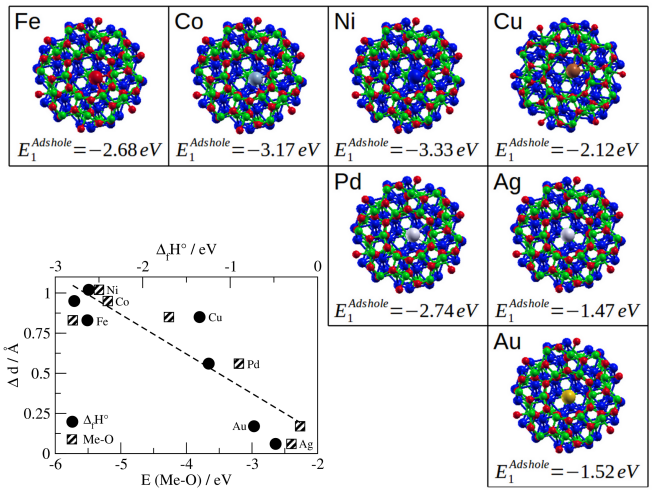

Fig. 2 Final configurations and adsorption energies of one metal atom inside the hole. Red, O atoms; green, Al; blue, Ni. In the plot, lateral displacement (Δd) as a function of $\Delta_f H°$ of oxides and of the Me-O molecule binding energy; the dashed line is a linear fit.

The adsorption energy, as well as the position with respect to the center of the hole, are different for each species. It has been previously shown that the interaction of Cu with the oxygen from the oxide is, among other factors, determining its position.[31] The affinity of the metallic species to oxygen, given for instance by the enthalpies of formation of the related oxides, could drive the displacement from the center of the hole towards the alumina, since the system gains energy when the oxidable metallic one-atom seed attaches to the oxygen atoms at the border of the defect. We have found indeed a correspondence between the lateral displacement (Δd) and the oxidability, given either by the magnitude of the enthalpies of formation of the corresponding oxides from existing literature data,[32–34] or by the calculated binding energy of the Me-O molecule: the stronger the affinity to oxygen (Fe, Co, Ni), the larger the displacement, as shown in Figure 2.

Beside the affinity to oxygen, other factors play a role in the stability of the monoatomic seed. The hole is a confined space and the size of the metallic atoms is one of them. The upper panel of Figure 3 shows that the larger the covalent radius of the seeding atom, the weaker the adsorption. It is worth noting that the atoms with less affinity to oxygen are also the biggest ones, therefore concluding that these two factors act in the same direction in stabilising or destabilising the monoatomic seed in the hole.

The strength of the adsorption can be rationalized in terms of electronic properties, from the analysis of the charge density distribution and of the density of states. The lower panels of Figure 3 show the adsorption energies as a function of the center of the d-levels of the metallic one-atom seeds adsorbed in the hole: metals with weaker binding, as Ag and Au, have their d-levels located at lower energies. The low position of the d-level makes some anti-bonding levels to be filled,[35] weakening the bonding. Conversely, metals which attach stronger to the hole have their d-levels placed at higher energies, closer to the Fermi level.

The net charge transfer between the seeding metal atoms and the support is not enough to explain their different behavior. The hole is always charged as expected, i.e., O layers negatively, Al layers positively charged, but the charge of the adsorbed metals varies without showing a clear trend: Pd and Ni monoatomic seeds are negatively charged; Au is slightly negative; Ag, Co and Fe are positive, and the Cu seed is practically neutral. It is more instructive, instead, to investigate the rearrangement of the charge density. Charge density difference plots are reported here only for Ni and Ag, which have the strongest and the weakest bonding inside the hole, respectively. This quantity is calculated by subtracting the charge density of the components (alumina/Ni_3Al substrate and a single metallic atom) to the charge density of the entire system. Figure 4a clearly shows the bonding with the underlying alloy and with the oxide in the case of Ni, and only a covalent bonding with the alloy in the case of Ag.

The adsorption energy of the metallic monoatomic seed is due to both the interaction with the underlying alloy and with the oxide, but clearly with different weights. To quantify these contributions, we have calculated the adsorption energy of the metallic atoms to the bare $Ni_3Al(111)$ alloy layer, in the same configuration they adopt when the oxide is present. In Figure

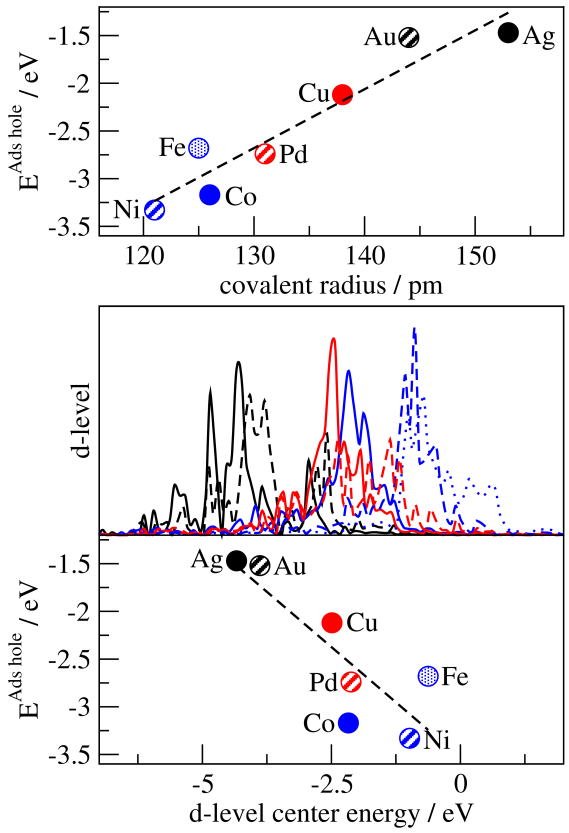

Fig. 3 Adsorption energy in the hole ($E^{Ads\ hole}$) as a function of the covalent radius (up) and the d-level center (bottom) for all the metals considered.

4b the difference:

$$\Delta E_{h-a} = E^{Ads\ hole} - E^{Ads\ alloy} \quad (2)$$

is shown for all the metals studied, where $E^{Ads\ alloy}$ is the adsorption energy in the bare alloy.

First of all we notice that the adsorption in the hole is mostly due to the bonding with the alloy, being at least as strong as 1.5 eV in the worst cases of Ag and Au, whereas the interaction with the oxygen of the oxide modifies it at most by 0.8 eV in case of Au and much less in all the other cases.

In the case of the most oxidable species, like Fe, Co and Ni, with formation enthalpy of the oxide larger than 2 eV per O atom (in absolute value), this difference is negative, indicating that the interaction with the oxide stabilizes the bond. On the other hand, for metals which clearly do not have a tendency to oxidation, as Au, the presence of the oxide is a destabilizing factor. These non-oxidable metals tend to stay far from the oxide but, being confined in the hole, at most they can stay in the center, as previously discussed, where they still interact with the oxide because of their large size. The interaction is repulsive, resulting in positive values of ΔE_{h-a}. It should be kept in mind that the preferable adsorption site for all the metallic species on the bare alloy would not be the center of the hole, on top of the Al atom of the underlying alloy, but in a hollow site. The position of the one-atom seeds is thus determined by an interplay between the interaction with the alloy, with the oxide and the confinement inside the hole.

Finally, we conclude the discussion about the attachment in the hole observing that the adsorption energy of Ag, Au, Cu is in line with the trend towards clusterization in the "*dot*" superstructure reported in[22]: the stronger the adsorption energy, the higher the degree of order observed also at high coverage.

3.2 Adsorption of metal atoms in the "*network*" site

The other preferential nucleation site observed for some metals is the *"network"*, which is a triangular site delimited by three oxygen atoms (see Figure 1). There are two "*network*" sites per unit cell, separated by 2.6 nm (those appearing as darker depressions when imaged at a bias of +3.2 eV), creating a honeycomb-like superstructure.

We have calculated the adsorption energy for the seven metal species in three positions on the "*network*": *on-top* of an O atom, in a *bridge* position, and in the center of the triangle (*hollow*). The adsorption sites and corresponding energies are shown in Figure 5.

The adsorption on the "*network*" is stable for all the metals studied (negative energies), and the preferential configuration is the *bridge* position, as reported for Cu,[31] breaking the symmetry of the system. It is stronger in the case of metals which tend to oxidize, as Fe, Co and Ni. For some metals, the differences in adsorption energy among different adsorption configurations on the "*network*" is negligible, as in the case of Au, and this may be as a consequence of the small affinity of this metal to oxygen.

To generate an ordered array of nanoclusters by self-assembly, it is necessary that the metallic atoms deposited through CVD adsorb preferentially only in one of the sites on the surface, generating seeds geometrically dispersed, and that the adsorption energy in that site is strong enough.

In Figure 6 we report for the various elements the differences in adsorption energies between the "*network*" and the "*dot*" sites:

$$\Delta E_{n-h} = E^{Ads\ net} - E^{Ads\ hole} \quad (3)$$

where $E^{Ads\ net}$ is the adsorption energy in the *bridge* position of the "*network*" site, as a function of the former, with reversed sign.

The adsorption inside the hole is preferred for all the metals considered, since ΔE_{n-h} is positive. Fig. 6 emphasises that Au and Pd are different from the other elements, since the diagonal distinguishes the elements where ΔE_{n-h} is smaller or

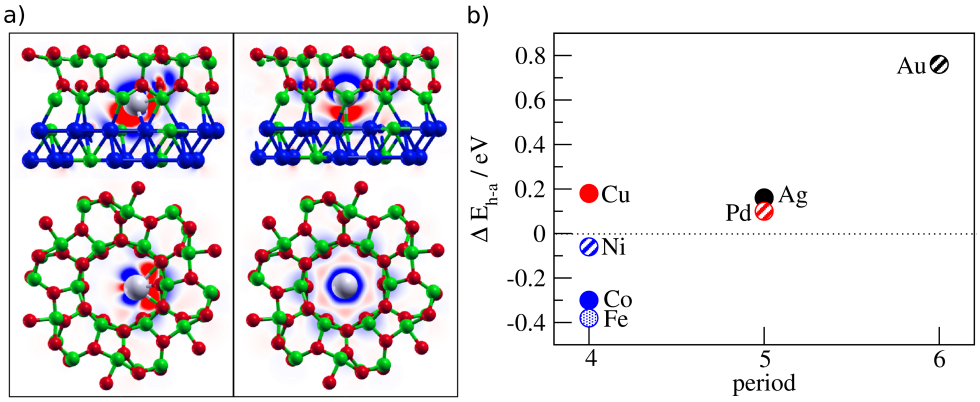

Fig. 4 a) Charge density difference plots (lateral and frontal planes containing the metal seed) showing bonding between the metal and the substrate. The atoms adsorbed (large white balls) are Ni (left) and Ag (right). Red balls, O atoms; green, Al; blue, Ni. Red areas in the charge density difference plots indicate electronic density accumulation; blue color, depletion. The range is between $\pm$ 0.0025 $|e|/a_B^3$. b) Adsorption energy difference between the metal in the full Al_2O_3/Ni_3Al substrate and on the bare alloy. Positive values mean destabilization in the presence of the oxide.

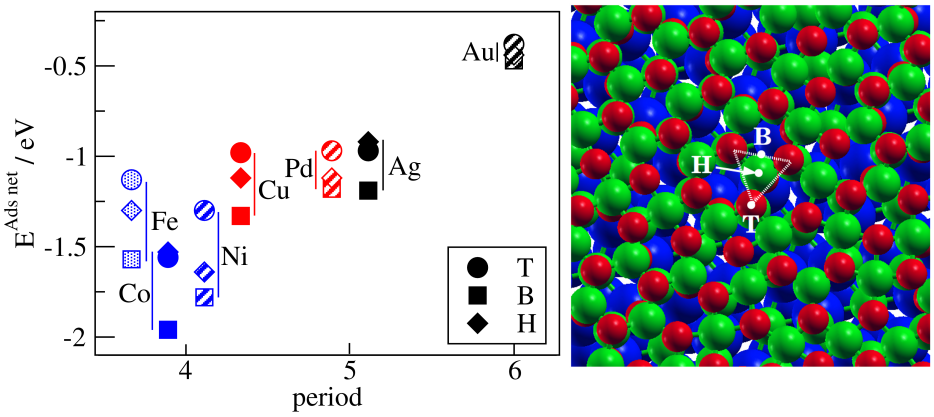

Fig. 5 Adsorption energies for the metal atoms on the different configurations on the "*network*" structure: T, *on-top* of an O atom; B, in a two-coordinated *bridge* position; H, in the three-coordinated *hollow* site. Red balls, O atoms; green, Al; blue, Ni.

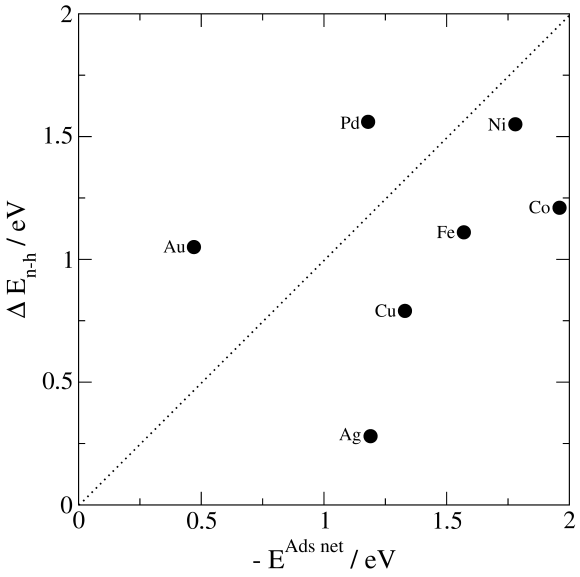

Fig. 6 Adsorption energy difference between the atoms in the best position of the "*network*" site and inside the hole, as a function of the former, with reversed sign.

larger than $|E^{Ads\ net}|$. For Au and Pd, $\Delta E_{n-h} > |E^{Ads\ net}|$, i.e. $|E^{Ads\ hole}| > 2|E^{Ads\ net}|$, corresponding to a strong preference for the "*dot*" site rather than the "*network*" site. However, Au cannot be used to create ordered seeds in the holes of the alumina, since its adsorption energies in the "*network*" and also in the "*dot*" sites are rather weak (position above the diagonal, on the left in the plot). Pd seems the best choice, since it has a strong difference between the adsorption energies in the two sites and it also has strong adsorption energy values in both sites (position above the diagonal, on the right). On the other hand, Ag would be the worst choice because there will be a competition between adsorption inside the "*dot*" and in the "*network*", accompanied by small values of the adsorption energies in both sites (position below the diagonal, on the left). Indeed, it was experimentally reported that Pd is a good choice for creating a seed inside the hole and for further proceeding with nucleation of another desired metal [19,26,27]. Conversely, it was reported that when Ag is deposited through CVD on alumina/$Ni_3Al(111)$ in big quantities, agglomeration of the clusters is observed: [22] although we are totally far from the high coverage regime, this behavior can be partially ascribed to the competition of different adsorption sites for Ag and to the relatively low adsorption strength.

Kinetic effects may also play an important role in the nucleation of different metals on the substrate. We have calculated the diffusion barriers for Ni and Pd on a selected path on the alumina surface ($T_1H_3T_1$ in Ref. [31]), and we have found values of 0.90 eV for Ni and 0.32 eV for Pd. Together with the previously calculated value of 0.45 eV for Cu, [31] we can explain the order Ni>Cu>Pd in the diffusion barriers by the affinity of the metals towards oxygen. The atoms which attach stronger to the oxide will hardly diffuse, and atoms arriving randomly through CVD would find more difficult to reach the preferential nucleation sites. This fact could explain why Pd is a much better seed than Ni, although thermodynamics favours both of them.

3.3 The palladium case

We have offered a rationale to what has been previously reported in the literature: [19,26,27] Pd is one of the best candidates to create self-assembled ordered seeds on the alumina thin film. The first atom adsorbs deep inside the hole with an energy of -2.74 eV, and the energy difference ΔE_{h-n} when comparing to the adsorption in the "*network*" is -1.56 eV. This difference allows to assume that all the Pd deposited through CVD will be adsorbed in the "*dot*" superstructure.

In order to investigate in details the adsorption in the defect, we have considered first of all the potential energy for a single Pd atom descending vertically inside it, following the same path examined for Cu. [31] This may not be the minimum energy path, but it allows to obtain an upperbound for the energies involved. The profile, shown in Figure 7 as a function of the height, shows that in the case of Pd there is no activation barrier along this path. The height is referred to the average position of the oxygen atoms in the outermost ionic layer of the oxide. For further reference, the average positions of the other ionic layers of the alumina, as well as the Ni_3Al alloy, are also indicated (colored stripes).

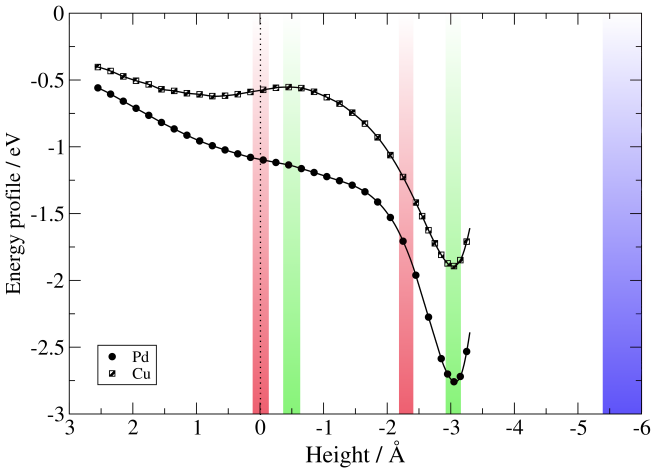

Fig. 7 Energy profiles of a Pd atom (dots) and a Cu atom (squares) descending vertically inside the hole of the alumina film as a function of its height. The zero is set at the position of the outermost layer of the oxide.

It is interesting to understand how the nucleation proceeds

further. When a second atom is introduced in the defect, two possible configurations for the seed are possible, as previously reported for Cu:[31] in the first one, the two atoms are in a vertical-like configuration, and in the second case, both atoms are in the bottom of the hole, attached to the underlying alloy. The adsorption energy of the *N*th Pd atom, which can be thought as the energy gained after adding this last Pd atom to the seed, can be estimated as:

$$E_N^{Ads\ hole} = E_{Subs+NPd} - E_{Subs+(N-1)Pd} - E_{Pd} \quad (4)$$

where $E_{Subs+NPd}$ is the energy of the complete system and $E_{Subs+(N-1)Pd}$ is the energy of the defect with *(N-1)* Pd atoms adsorbed in the most stable positions. In addition, the average adsorption energy can be calculated as:

$$< E_{Ads} >= E_{Subs+NPd} - E_{Subs} - NE_{Pd} \quad (5)$$

These configurations, with the corresponding adsorption energies, are shown in Figure 8.

For the 2-atoms case, the main difference with Cu is that for Pd the configuration with the two atoms in the bottom of the hole is much less stable than the vertical-like structure. This may be due to the larger covalent radius of Pd (the equilibrium distance of a Pd_2 molecule in vacuum is 2.48 Å while the equilibrium distance of a Cu_2 molecule is 2.22 Å) and its lower affinity to oxygen; the interaction with the oxide is minimized in the vertical-like configuration.

After adding a third Pd atom, again two stable adsorption geometries have been found. One of them consists of two atoms deep inside the hole as a dimer, and the third one attached to them in a *bridge* position. The other seed is a vertical-like one, which has been found to be more stable, with an average adsorption energy of -2.00 eV per Pd atom, and its stability could be also described in terms of the minimization of the repulsion with the oxide. This is indeed the configuration of the seed proposed in a previous work,[19] that is confirmed to be the most favored by our calculations.

Surprisingly, more than three Pd atoms can be accommodated inside the hole, as shown in Figure 8. We have found that it is possible to grow seeds made up to 6 Pd atoms. Particularly, the 5-atoms case seems to be quite stable. The 6-atoms seed is thermodynamically stable considering only globally the attachment of the entire seed to the hole, although only 0.21 eV are gained when adding the 6th atom (taking as a reference the 5-atoms seed).

In all the cases, the mechanism of seeding will be of much importance. If the seed is created atom by atom (and there are no dimers diffusing and entering the hole), there will always exist a competition for further Pd atoms between anchoring at the "*dot*" sites ($E_N^{Ads\ hole}$, with $N > 1$) or at the "*network*" site ($E^{Ads\ net} = -1.18$ eV). In some seed configurations the energy gained after adsorbing the *N*th atom is lower than the adsorption energy on the empty "*network*" and probably these configurations will be more rare to occur. As an example, if the 5-atoms seed is already formed, the energy gained when adding the 6th atom to the seed is much lower than the energy the system would gain if the 6th Pd atom attaches to the "*network*".

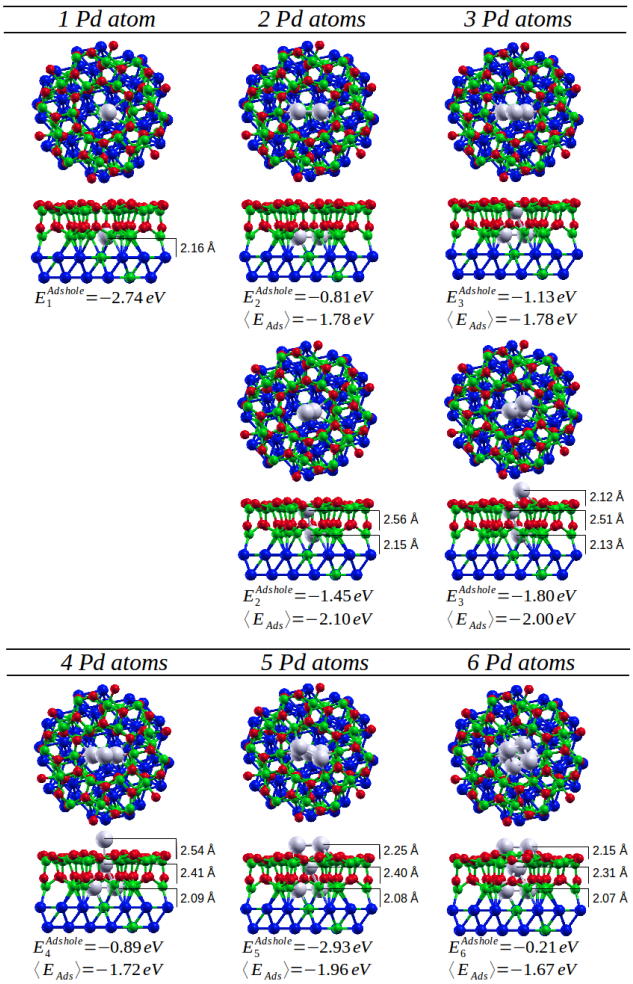

Fig. 8 Equilibrium configurations for Pd seeds on $Al_2O_3/Ni_3Al(111)$ composed of up to six atoms. Adsorption energies are indicated (see the text for details). Red balls, O atoms; green, Al; blue, Ni; white, Pd.

4 Conclusions

We have studied the seeding of seven transition metal species on the $Al_2O_3/Ni_3Al(111)$ substrate. Two preferential sites have been considered: inside the holes defining the "*dot*" superstructure and in the "*network*".

For all the considered metals, adsorption inside the holes

is always preferred. In this position, the metallic one-atom seeds attach deep inside the defect and in the case of oxidable metals, lateral displacement is observed in order to gain stabilization by interaction with the oxide. In the case of large and non-oxidable metals, repulsion exists with the borders of the oxide, and no lateral displacement is observed, as a way to avoid interaction with the oxygen ions.

Adsorption in the "*network*" superstructure is also stable, and the preferred configuration is a *bridge* position. Nevertheless, adsorption inside the holes is always thermodynamically favoured.

By considering the differences in adsorption energies between the "*dot*" and the "*network*" sites, we give a rationale for the experimentally observed different behavior of metals nucleating on this substrate. Ag is indeed the worst choice to create an ordered pattern of seeds, having the smallest adsorption energy difference between the two positions. Conversely, Pd and Ni are the most promising metals to create highly ordered seeds, due to the strong preference towards the holes. We have deserved special attention to Pd since, accounting also for kinetics, it is the best candidate: its lower affinity to oxygen makes it very easily diffuse on the oxide surface and reach the holes. We have extended therefore our study to bigger Pd seeds thermodynamically stable inside the holes. Up to 6 atoms can be accommodated in the defects. Further addition of Pd would give rise to ordered nanoclusters.

The ab-initio approach used here is very reliable to describe the details of the chemical bonding of the individual atoms with the oxide but it is limited to the study of systems with few hundreds of atoms, configurations close to equilibrium and at 0 K, and cannot be used to study the real dynamics of the synthesis process of NPs. However, the role of temperature and of the CVD deposition rate in the complete process is an issue that goes beyond the scope of the present work, devoted to the deep understanding of the first stages of the growth.

5 Acknowledgments

We acknowledge financial support from: Italian Ministry of University and Research through Futuro in Ricerca, FIRB 2010 project RBFR10J4H7; Italian Ministry of Foreign Affairs and International Cooperation (MAECI), Directorate General for the Country Promotion, through the Executive Programme with Argentina; Consortium for Physics of Trieste, Italy. Computational resources have been partly obtained through Italian Super-Computing Resource Allocation (ISCRA) grants of the Consorzio Interuniversitario CINECA, partly within the agreement between the University of Trieste and CINECA.

References

1 R. Ferrando, J. Jellinek and R. L. Johnston, *Chemical Reviews*, 2008, **108**, 845–910.
2 B. L. M. Hendriksen and J. W. M. Frenken, *Phys. Rev. Lett.*, 2002, **89**, 046101.
3 K.-i. Shimizu and A. Satsuma, *Phys. Chem. Chem. Phys.*, 2006, **8**, 2677–2695.
4 R. Westerstrm, J. G. Wang, M. D. Ackermann, J. Gustafson, A. Resta, A. Mikkelsen, J. N. Andersen, E. Lundgren, O. Balmes, X. Torrelles, J. W. M. Frenken and B. Hammer, *Journal of Physics: Condensed Matter*, 2008, **20**, 184018.
5 G. Rupprechter and C. Weilach, *Journal of Physics: Condensed Matter*, 2008, **20**, 184019.
6 H. Over, O. Balmes and E. Lundgren, *Surface Science*, 2009, **603**, 298 – 303.
7 J. J. McClelland, R. E. Scholten, E. C. Palm and R. J. Celotta, *Science*, 1993, **262**, 877–880.
8 P. Avouris, *Accounts of Chemical Research*, 1995, **28**, 95–102.
9 A. N. Shipway, E. Katz and I. Willner, *ChemPhysChem*, 2000, **1**, 18–52.
10 H. Brune, M. Giovannini, K. Bromann and K. Kern, *Nature*, 1998, **394**, 451–453.
11 S. Y. Shiryaev, F. Jensen, J. L. Hansen, J. W. Petersen and A. N. Larsen, *Phys. Rev. Lett.*, 1997, **78**, 503–506.
12 U. Bardi, A. Atrei and G. Rovida, *Surface Science*, 1990, **239**, L511 – L516.
13 U. Bardi, A. Atrei and G. Rovida, *Surface Science*, 1992, **268**, 87 – 97.
14 C. Becker, J. Kandler, H. Raaf, R. Linke, T. Pelster, M. Drager, M. Tanemura and K. Wandelt, author, 1998, pp. 1000–1005.
15 A. Rosenhahn, J. Schneider, J. Kandler, C. Becker and K. Wandelt, *Surface Science*, 1999, **433435**, 705 – 710.
16 R. Franchy, *Surface Science Reports*, 2000, **38**, 195 – 294.
17 A. Rosenhahn, J. Schneider, C. Becker and K. Wandelt, author, 2000, pp. 1923–1927.
18 S. Degen, A. Krupski, M. Kralj, A. Langner, C. Becker, M. Sokolowski and K. Wandelt, *Surface Science*, 2005, **576**, L57 – L64.
19 M. Schmid, G. Kresse, A. Buchsbaum, E. Napetschnig, S. Gritschneder, M. Reichling and P. Varga, *Phys. Rev. Lett.*, 2007, **99**, 196104.
20 E. Vesselli, A. Baraldi, S. Lizzit and G. Comelli, *Phys. Rev. Lett.*, 2010, **105**, 046102.
21 A. Wiltner, A. Rosenhahn, J. Schneider, C. Becker, P. Pervan, M. Milun, M. Kralj and K. Wandelt, *Thin Solid Films*, 2001, **400**, 71 – 75.
22 C. Becker, A. Rosenhahn, A. Wiltner, K. von Bergmann, J. Schneider, P. Pervan, M. Milun, M. Kralj and K. Wandelt, *New Journal of Physics*, 2002, **4**, 75.
23 A. Lehnert, A. Krupski, S. Degen, K. Franke, R. Decker, S. Rusponi, M. Kralj, C. Becker, H. Brune and K. Wandelt, *Surface Science*, 2006, **600**, 1804 – 1808.
24 M. Marsault, G. H. A. Worz, G. Sitja, C. Barth and C. R. Henry, *Faraday Discuss.*, 2008, **138**, 407–420.
25 A. Buchsbaum, M. De Santis, H. C. N. Tolentino, M. Schmid and P. Varga, *Phys. Rev. B*, 2010, **81**, 115420.
26 G. Hamm, C. Becker and C. R. Henry, *Nanotechnology*, 2006, **17**, 1943.
27 S. Degen, C. Becker and K. Wandelt, *Faraday Discuss.*, 2004, **125**, 343–356.
28 P. Giannozzi, S. Baroni, N. Bonini, M. Calandra, R. Car, C. Cavazzoni, D. Ceresoli, G. L. Chiarotti, M. Cococcioni, I. Dabo, A. D. Corso, S. de Gironcoli, S. Fabris, G. Fratesi, R. Gebauer, U. Gerstmann, C. Gougoussis, A. Kokalj, M. Lazzeri, L. Martin-Samos, N. Marzari, F. Mauri, R. Mazzarello, S. Paolini, A. Pasquarello, L. Paulatto, C. Sbraccia, S. Scandolo, G. Sclauzero, A. P. Seitsonen, A. Smogunov, P. Umari and R. M. Wentzcovitch, *Journal of Physics: Condensed Matter*, 2009, **21**, 395502.
29 D. Vanderbilt, *Phys. Rev. B*, 1990, **41**, 7892–7895.

30 J. P. Perdew, K. Burke and M. Ernzerhof, *Phys. Rev. Lett.*, 1996, **77**, 3865–3868.
31 J. A. Olmos-Asar, E. Vesselli, A. Baldereschi and M. Peressi, *Phys. Chem. Chem. Phys.*, 2014, **16**, 23134–23142.
32 B. J. Boyle, E. G. King and K. C. Conway, *Journal of the American Chemical Society*, 1954, **76**, 3835–3837.
33 H. Shi, R. Asahi and C. Stampfl, *Phys. Rev. B*, 2007, **75**, 205125.
34 J. Yan and J. K. Nørskov, *Phys. Rev. B*, 2013, **88**, 245204.
35 B. Hammer and J. K. Norskov, *Nature*, 1995, **376**, 238–240.